INTERNATIONAL JOURNAL OF CLIMATOLOGY
Int. J. Climatol. (2017)
Published online in Wiley Online Library
(wileyonlinelibrary.com) DOI: 10.1002/joc.5163

Changing patterns of daily precipitation totals at the Coweeta Hydrologic Laboratory, North Carolina, USA

T. P. Burt,[a*] C. Ford Miniat,[b] S. H. Laseter[b†] and W. T. Swank[b]
[a] *Department of Geography, Durham University, UK*
[b] *USDA Forest Service, Southern Research Station, Coweeta Hydrologic Lab, Otto, NC, USA*

ABSTRACT: A pattern of increasing frequency and intensity of heavy rainfall over land has been documented for several temperate regions and is associated with climate change. This study examines the changing patterns of daily precipitation at the Coweeta Hydrologic Laboratory, North Carolina, USA, since 1937 for four rain gauges across a range of elevations. We analyse seasonal total rainfall, number of rain days and the frequency of heavy rainfall. We compare these with several teleconnections, including the Bermuda High Index (BHI), the West BHI, the North Atlantic Oscillation (NAO) and the El Niño-Southern Oscillation. Our data show a tendency for increased variability, including major periods of drought, with fewer rain days recently, especially in summer. Only autumn tended to have increases in rainfall frequency and magnitude; this is the season when orographic enhancement is at its strongest. The major driver of precipitation at Coweeta is the strength of the Bermuda High. The strength of the NAO is important in summer. The results are relevant to the southeast United States in general, given that the region comes under the influence of similar air masses during the year. The findings are applicable to the wider Appalachian Mountains and to other mountainous regions where there is significant orographic enhancement.

KEY WORDS rainfall; Coweeta; orographic enhancement; Bermuda High

Received 1 September 2016; Revised 8 May 2017; Accepted 10 May 2017

1. Introduction

Globally, precipitation extremes are increasing, a result of increasing air temperatures at low elevations leading to increased evaporation and higher water vapour content in the atmosphere (Meehl *et al.*, 2007; Allan and Soden, 2008; O'Gorman and Schneider, 2009; Hartmann *et al.*, 2013). Because of the dependence of the saturation water vapour pressure on temperature, as predicted by the Clausius–Clapeyron equation), a 1 °C temperature increase leads to an approximate 7% increase in the moisture-holding capacity of the atmosphere. Since about 1950 the number of heavy precipitation events over land has increased, and in North America the frequency or intensity of heavy precipitation has increased, depending on season and region (Hartmann *et al.*, 2013). Since 1910, precipitation across the United States has increased by about 10%, again due to increases in the frequency and intensity of very large precipitation events, with the proportion of total annual precipitation derived from heavy rainfall increasing (Karl and Knight, 1998). This pattern of increasing frequency and intensity of heavy rainfall holds true for the southern Appalachian region within the United States as well (Karl and Knight, 1998). Changes in the proportion of precipitation derived from heavy rainfall (variation) without a proportional increase in the total annual rainfall (mean) must result in increases in the number of dry days. Indeed, for the southeast (SE) United States a significant increase in dry days during summers is occurring along with increases in heavy rainfall events (Wang *et al.*, 2010). Such variability in dry days has been attributed to changes in the location and intensity of the western ridge of the North Atlantic ('Bermuda') subtropical high (Li *et al.*, 2011) and in the greater variability in the North Atlantic Oscillation (NAO) since about 1950 (Hurrell *et al.*, 2003).

The NAO is an important mode of climatic variability in the Northern Hemisphere including the eastern United States (Hurrell *et al.*, 2003; Folland *et al.*, 2009). The strength and position of the NAO varies seasonally, generally expanding over much of the North Atlantic during winter and contracting and shifting poleward during summer. Summer streamflow east of the Appalachians from New England to the Gulf of Mexico is positively correlated with the strength of the NAO (Coleman and Budikova, 2013). A tendency for drier summers in the southern Appalachians (Laseter *et al.*, 2012) might therefore be associated with a long-term decline in summer NAO since the middle of the 20th century. NAO is in part affected by the behaviour of the Bermuda High, as the NAO depends both on the Bermuda High and the Icelandic Low. Diem (2013) notes that the Bermuda High Index (BHI) had a significant positive trend from the 1970s to 2009, and the western ridge of the Bermuda High moved

* Correspondence to: T. P. Burt, Department of Geography, Durham University, Durham DH1 3LE, UK. E-mail: t.p.burt@durham.ac.uk

† Current address: USDA Forest Service, Southern Research Station, Center for Integrated Forest Science, Franklin, NC, USA.

significantly south-eastward from approximately the mid-1970s–2009.

Complex terrain can also influence precipitation totals, through orographic enhancement and interactions with cloud and fog layers. Integrated analysis of model simulations and observations have demonstrated how low-level feeder–seeder interactions play an important role in orographic enhancement in the southern Appalachians (Hill *et al.*, 1981; Wilson and Barros, 2014). Rainfall at higher elevations is characterized by higher rainfall intensity. This is particularly important in the cooler seasons when convective activity is less vigorous (Prat and Barros, 2010). Stratiform rainfall systems can also interact with local low-level clouds and fog, the latter being persistent at high altitudes in this region (Wilson and Barros, 2014). This can help account for systematic differences in rainfall totals between valley locations and ridge tops. On the other hand, the passage of warm-season intense storm systems including tropical depressions and cool-season synoptic-scale storms may produce rainfall distributions much less well correlated with topography. Localized thunderstorm activity would have the same effect, possibly even favouring (warmer) valleys over (cooler) ridge tops if the valleys are where the storm cells are generated. Interesting diurnal variations emerge seasonally with more afternoon rainfall in summer, as might be expected.

Orographic controls on precipitation can also interact with larger-scale climate modes. For example, Coleman and Budikova (2013) suggest that in summer, when the NAO is positive, orographic uplift and local convection occur along the east side of the Appalachians. For the British Isles, Burt and Howden (2013) showed that variations in the strength of the NAO, in this case influenced mainly by the strength of the Icelandic Low, cause large differences in seasonal precipitation totals compared to NAO-neutral conditions, an effect which is amplified with altitude – what Burt and Howden (2013) term 'double orographic enhancement'. Similar effects have been noted for the mountains of the Pacific Northwest United States and Sri Lanka, both linked to variations in the El Niño-Southern Oscillation (ENSO: Burt and Howden, 2013). In all such cases, it is the movement of storm systems across the upland area which is important in generating the orographic effect. Hurrell and VanLoon (1997) and Burt *et al.* (2014) emphasize that studies of long-term trends of temperature or precipitation in local climate records, especially those from high-elevation sites, should also examine parallel changes in atmospheric circulation in order to fully synthesize the available information about regional or global climate change.

Our purpose here is to analyse the long-term, *daily* precipitation records at the Coweeta Hydrologic Laboratory, one of the wettest locations in SE United States. Coweeta is among the oldest, continuously operating environmental study sites in North America (Swank and Crossley, 1988; Laseter *et al.*, 2012). Coweeta has observed increased precipitation variability in recent decades with summer months becoming drier over time and autumn months becoming wetter (Laseter *et al.*, 2012). Given its location in the SE United States, Coweeta is particularly influenced by atmospheric conditions prevailing across the Atlantic Ocean. Our analysis includes examining variation with altitude, and possible drivers such as the Bermuda High and the NAO, including the possible amplification of precipitation totals at high altitude. Given Coweeta's location, it is anticipated that the Bermuda High will be a major driver of precipitation, with a more direct linkage compared to the NAO, However, we also include other climatic indices to investigate whether other teleconnections might exist, in particular links to conditions in the Pacific Ocean. The findings may be relevant to other mountainous regions which are subject to significant orographic enhancement driven by strong atmospheric circulation across a topographic barrier.

2. Site description and methods

2.1. Study site

The USDA Forest Service, Coweeta Hydrologic Laboratory (2185 ha) lies in the Nantahala Mountains of western North Carolina, USA (35°03′N, 85°25′W: Figure 1). Established in 1934, it has been a testing ground for theoretical and applied forest hydrological research (Swank and Crossley, 1988). Climate in the Coweeta Basin is classified as perhumid, mesothermal with water surplus in all seasons (Swift *et al.*, 1988). Precipitation comprises frequent, low-intensity rain in all seasons with little snow. Occasional intense storms are associated with severe thunderstorms or inland influences from hurricanes (Shepherd *et al.*, 2007). For all rain-gauge sites at Coweeta, March is the wettest month (193 mm) and October is the driest (112 mm).

2.2. Daily precipitation measurements

Long-term climate and precipitation have been monitored at Coweeta through a network of gauging stations at different elevations and aspects since 1934 (Swift *et al.*, 1988). Parameters include temperature, rainfall, wind speed and direction, humidity, solar radiation, air quality and evaporation. A network of 12 standard rain gauges (SRG, 8-in. Standard Rain Gauge, National Weather Service) and nine recording rain gauges (RRG, Belfort Universal Recording Rain Gauge, Belfort Instrument Co., Baltimore, MD, USA) are currently located throughout the basin; four recording rain gauges are included in this study (Table 1). Total precipitation is measured by the SRG; volume and intensity are measured by the RRG. The longest running climate station is CS01 at the valley floor, with a co-located recording rain gauge (RRG06). Here, measurements started in 1937. CS01 is also a cooperative station with the National Weather Service. Measurements at the other three (higher-altitude) gauges started as follows: RG13 (1942), RG96 (1943) and RG31 (1958). Complete daily records exist for all four gauges from the start date to present. There is some doubt about the problem of under-catch, in two regards. Hibbert (1966, quoted in Swift *et al.* 1998) noted that precipitation totals increase

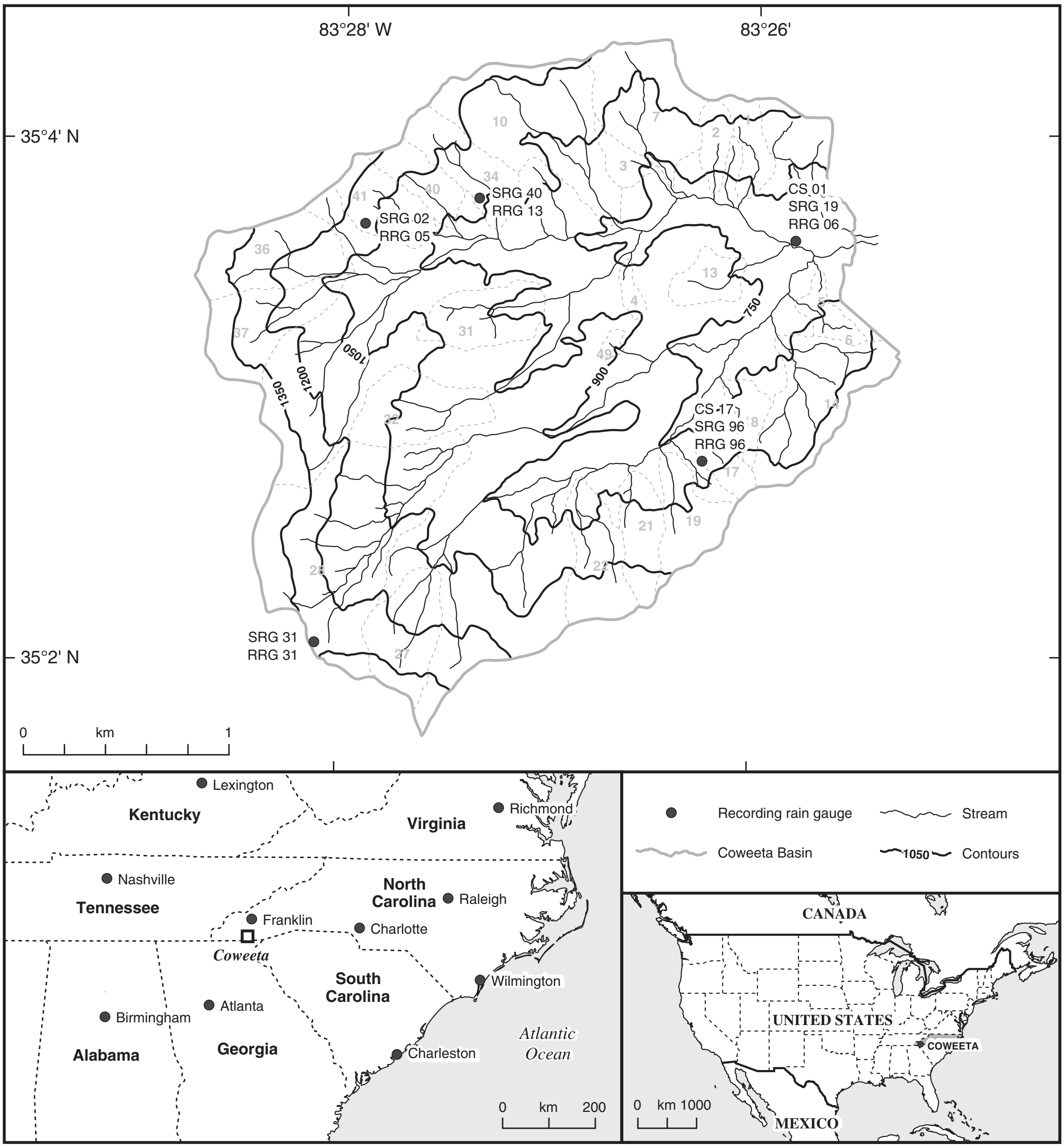

Figure 1. The location of the Coweeta Hydrologic Laboratory.

fairly regularly with altitude except near ridge-tops where catch was significantly lower than immediately downslope: reductions of about 30% in a 30 m change of elevation extending about 100 m either side of a ridge. It is possible therefore that totals at RRG31 are less than they should be. There is also some doubt about totals at RRG40 compared to RRG96 because of differential exposure in relation either to topography or shelter from nearby trees (see below). Of more significance is the problem of under-catch for the very lowest observed totals. Histograms of daily precipitation totals should show a smooth, negative exponential distribution but all four gauges show a lower total for catches of 0.254 mm (0.01 in.) compared to the next category 0.508 mm (0.02 in.). This is not likely to be a problem unique to Coweeta: e.g. at Oxford, England, there is the same under-catch for both hourly (tipping bucket) and daily (manual observation) data. Under-catch of the smallest amounts is not at all significant for long-period totals, given that such small amounts are involved, but may well be for counts (Burnette and Stahle, 2014). For that reason, the frequency of wet days (at least 1 mm total) is used here in subsequent analyses instead of rain days.

2.3. Precipitation analysis

Analysis of heavy rainfall, as indicated by daily totals, follows Osborn *et al.* (2000) and Maraun *et al.* (2008). We ranked all daily rainfall data, accumulating the totals and identified the group of highest daily totals that together contributed 10% of the total precipitation (henceforth

Table 1. Location, elevation and first record of recording gauges included in this study (partly based on Laseter *et al.* 2012).

Recording gauge (RRG)	Paired standard gauge (SRG)	Elevation (m)	Start of record	Aspect	T10 (mm)
06	19	685	1 January 1937	Valley bottom	74.9
96	96	894	1 January 1944	North-facing	79.5
40	13	961	1 January 1943	South-facing	78.5
31	31	1366	1 January 1959	High-elevation gap	90.9

T10). Following Osborn *et al.* (2000), the cumulative rainfall totals are only calculated for rain days, defined as a day with total of 0.25 mm or more. For a long daily rainfall series, only a very small fraction of total rainfall is thereby excluded. T10 values for the four gauges are listed in Table 1; they range from 74.9 mm at the lowest gauge to 90.9 mm at the highest. Other precipitation thresholds examined include daily totals of 25 and 50 mm and the upper quartile (Q3) for all rain day totals at RRG06: 17.8 mm. Measures of dispersion include the lower quartile (Q1) and the upper quartile (Q3) and the 10th and 90th percentiles. Seasons are defined as: winter (December–February: DJF), spring (March–May: MAM), summer (June–August: JJA) and autumn (September–November: SON). Analyses for all four gauges started on 1 January for the first available complete year of record (Table 1) until 31 December 2012. We used 20-year moving windows (Burt *et al.*, 2008) to fit percentiles and quartiles to the data series ($n = 57$ for the moving-window correlations). We also use running monthly totals to identify major periods of below-average rainfall, as trends in accumulated deficit can be misleading (Linacre, 1992). Use of 24-month totals highlights more protracted droughts compared to short-term deficits. For analyses of orographic enhancement, because all rain gauges do not have the same length of record, we truncate the records for a common period (1959–2013) to allow comparison.

2.4. Regional atmospheric and sea surface temperature data

NAO data were obtained from the Climatic Research Unit (UEA CRU, 2015). The NAO is defined as the normalized pressure difference between a station on the Azores (Ponta Delgada) and one on Iceland (Reykjavik). Seasonal values of the BHI and the West BHI (WBHI) were obtained from Diem (2013). The BHI is an index of the difference between normalized sea-level pressure over Bermuda and New Orleans, Louisiana (Stahle and Cleaveland, 1992); seasonal sea-level pressure values are for grid cells corresponding to 32.5°N, 64°W and 30°N, 90°W. The centre of the Bermuda High is typically located approximately 2500 km east of Bermuda during summer; therefore, the BHI shows the standardized pressure gradient across the western side of the Bermuda High. The WBHI is based on the BHI; it uses 850-hPa heights and is centred over the SE United States. Seasonal 850-hPa geopotential heights are for grid cells corresponding to 30°N, 75°W and 30°N, 92°W (Diem, 2013). Other proxy measures of atmospheric circulation used here include the NINO12, NINO3 and NINO34 indices, which are measures of sea-surface temperature (SST) anomalies in the Pacific Ocean (Kaplan *et al.*, 1998) and the Pacific North America (PNA) index. The NAO index tends to be easier to interpret physically, but is based on only two arbitrary stations. PNA data (starts in 1950; $n = 63$ here), were downloaded (NOAA National Weather Service, 2015), as were extended SST anomaly data for equatorial regions of the Pacific based on Kaplan *et al.* (1998) (IRI LDEO, 2015). The regions included are the composite regions NINO12 (0°–10°S, 80°–90°W) and NINO34 (120°–170°W, 5°S–5°N) plus the core region NINO3 (150°–90°W, 5°S–5°N). We derive relationships between seasonal totals of precipitation statistics and averages of climatic indices using ordinary least squares regression. We also undertook a composite analysis (Bulic and Kucharski, 2012), identifying mean summer rainfall for all years that were more than ±1 standard deviation (SD) from mean summer NAO. We conducted a *t*-test on these composite data.

3. Results

3.1. Temporal and spatial patterns

While precipitation in the Coweeta Basin was not characterized by pronounced seasonality, seasonal differences did exist (Table 2). Although summer had the most rain days, winter was the wettest season; while autumn was the driest. Summer had the lowest mean rainfall per rain day and the lowest number of days with totals above 25 mm. The highest daily total (196.9 mm) was recorded on 4 October 1964.

There were almost no significant trends in rainfall regime in winter, spring and summer, but autumn has become wetter with heavier rainfall more common (Table 3). Laseter *et al.* (2012) noted a long-term increase in September rainfall totals, which is clearly a part of this autumn trend. RRG96 had significant positive trends in autumn for total rainfall plus the number of days above 25 mm and above the T10 mm threshold. RRG40 had positive trends only in autumn for the T10 mm threshold. It had negative trends for numbers of rain days per year and the number of days above 25 mm in winter; it also had significant negative trends for rain days in spring, summer and for the year as a whole. At the highest-elevation gauge, RRG31, there were significant trends for the number of days above 25 mm in winter (negative) and the number of days above the T10 in summer (positive). Note that, for all four gauges, other

Table 2. Mean rainfall total, mean number of days above given threshold values, maximum daily rainfall and mean rain per rain day by season at RRG06, 1937–2013.

	Winter	Spring	Summer	Autumn	Annual
Total (mm)	517	474	411	396	1799
Rain days	34	35	39	27	135
Days >17.8 mm (Q3)	10	9	7	7	34
Days >25 mm	7	6	4	5	22
Days >50 mm	2	2	1	2	6
Days >T10 per decade	6	4	3	6	19
Daily maximum (mm)	158.0	192.5	153.4	196.9	196.9
Rain/rain day (mm day^{-1})	15.0	13.6	10.5	14.6	13.3
Mean air temperature	4.2	12.7	21.3	13.3	12.9

Also shown is mean air temperature (°C). Note that some rows may not be exact totals due to rounding errors.

Table 3. Correlations for variables which changed significantly during the study period at the RRG06 rain gauge.

RRG06	Winter	Spring	Summer	Autumn	Annual
Total				0.258	
Wet days					
Days >17.8					
Days >25				0.267	
Days >50					
Days >T10				0.284	
Daily maximum (mm)				**0.339**	
Rain/rain day (mm day^{-1})				**0.335**	0.241
Mean air temperature (°C)		**0.427**	**0.447**	0.341	**0.459**

Correlations significant at $p < 0.05$ are shown in plain font, $p < 0.01$ in bold and $p < 0.001$ in bold and underlined ($n = 76$). Blank cells indicate no significant correlation. Note that significant correlations for the other three gauges are noted in the text but now shown in a table.

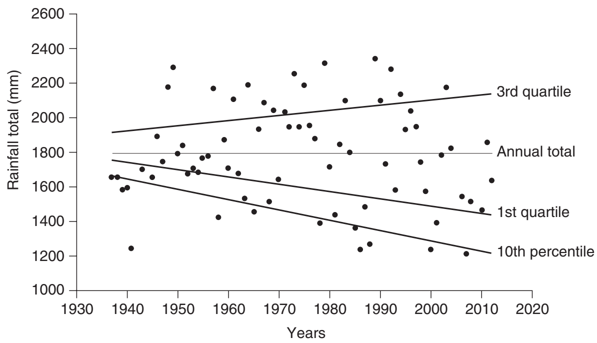

Figure 2. Increasing variability of annual rainfall totals at Coweeta (RRG06) over time. Trends for 10th percentile, IQ1 and IQ3 are statistically significant. Trends for annual total and 90th percentile (not shown) are not statistically significant.

than for T10, all the significant trends were negative except those in autumn which were uniformly positive. Results for the T10 index are of limited value given large numbers of zeroes in the record.

3.2. Variability

Laseter *et al.* (2012) noted a tendency for annual precipitation totals to become more variable over time, with wetter wet years and drier dry years. At RRG06 (Figure 2) there were downward trends ($p < 0.001$) for the 10th percentile ($r = 0.89$) and Q1 ($r = 0.77$), and an upward trend for Q3 ($r = 0.66$; Figure 2). Thus, variability over time increased, with increases in the inter-quartile range (IQR) over time ($r = 0.83$, $p < 0.001$). Up to 1974, only one year had a rainfall total more than one SD below the mean; since 1975 there were eight such years. Totals above one SD were similar, seven up to 1974, but only six since. Totals above two SDs increased from two to four in the latter half of the study period. Downward trends for the Q1 in winter, spring and summer ($r > 0.69$ and $p < 0.0001$; and for Q3 in winter ($r = 0.73$, $p < <0.0001$) and summer ($r > 0.32, p < 0.05$) were also observed. In contrast, autumnal Q1 and Q3 trended upward for total rainfall ($r > 0.77$ and $p < <0.0001$ for both seasons).

The IQR for numbers of wet days narrowed in winter ($r = -0.3$) and autumn ($r = -0.54$) but widened very significantly in summer ($r = 0.82$). Q1 for numbers of wet days fell significantly in all seasons except autumn and for the year as a whole ($r = -0.55$), but increased significantly in autumn ($r = 0.42$). Q3 for numbers of wet days decreased significantly in winter ($r = -0.54$) but increased significantly in summer ($r = 0.35$). The changing frequency of numbers of wet days very much accords with changes in totals, of course, especially in relation to wetter autumns and more variable summers. Negative trends in numbers of rain days in summer and for the year as a whole are not seen for numbers of wet days (Figure 3(b)). The results for numbers of rain days deserves further attention and might relate to warmer summers, a reduction in the occurrence of light showers, or some other cause. Comparison with other gauges across widely different climatic regimes could also be worthwhile.

3.3. Intensity

There was no trend for mean rainfall per day except in autumn ($r = 0.27$, $p < 0.05$), which also was the only season with a significant change (increase) in rainfall total over time (Table 3). Variation in mean rainfall per wet day (as indicted by IQR) also increased over time in both autumn ($r = 0.27$, $p < 0.05$) and for the year as a whole ($r = 0.46$, $p < 0.001$), whereas variation in summer

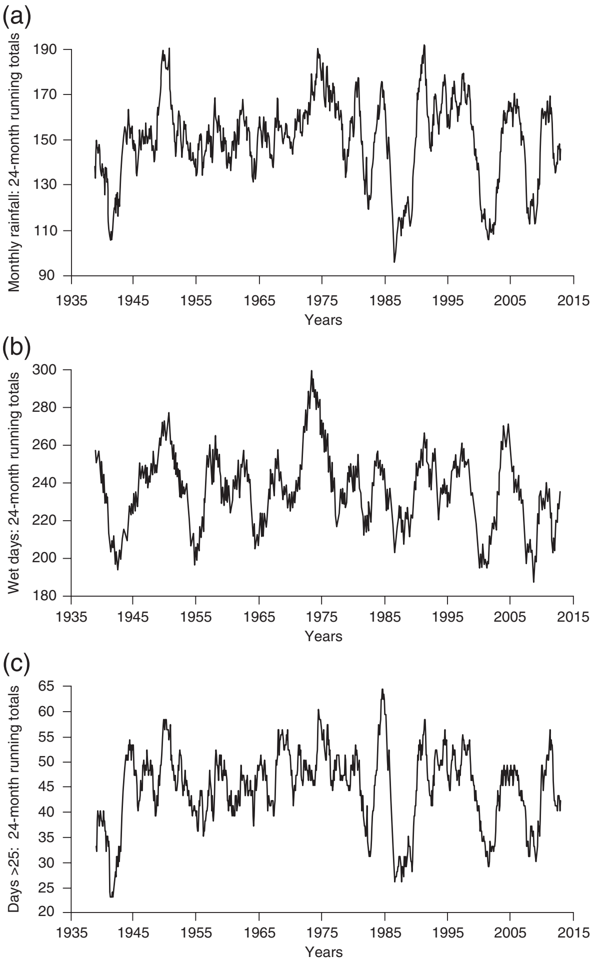

Figure 3. Twenty four-month running totals at RRG06 for (a) rainfall total, (b) wet days and (c) days with more than 25 mm.

decreased significantly ($r = -0.68$, $p < 0.0001$). There was no significant change in winter or spring.

Although the number of daily falls above 25 mm each year did not change significantly over the study period, variation increased over time (IQR, $r = 0.37$, $p < 0.01$). Autumn was the only season with a significant (positive) trend in numbers of daily totals above 25 mm (Table 4). All four measures of dispersion used here (Q1, Q3 and the 10th and 90th percentiles) and the IQR ($r = 0.596$, $p < 0.001$) increased in autumn over time. In summer, the Q3 and the 90th percentile increased whilst the 10th percentile decreased; accordingly the IQR increased ($r = 0.48$, $p < 0.001$). In winter all measures of dispersion decreased over time, but the IQR increased ($r = 0.32$, $p < 0.05$). Spring IQR decreased for numbers of days above 25 mm ($r = -0.43$, $p < 0.01$). The results for the upper quartile value 17.8 mm were very similar to those for the 25 mm threshold. Correlations for totals above 50 mm and for the T10 index were hampered by large numbers of zeroes, but numbers of T10 events increased in autumn ($r = 0.28$, $p < 0.05$). Maximum daily rainfall in autumn increased over the 76-year period of analysis ($r = 0.34$, $p < 0.01$), and the variability of heavy rainfall increased in all seasons except spring (Table 5). Autumn

Table 4. Mean annual data for the four recording rain gauges, 1959–2013.

	RRG06	RRG96	RRG40	RRG31
Total (mm)	1814	2010	1981	2394
Rain days	134	130	129	140
Days >25 mm	22	26	25	31
Days >50 mm	6	8	8	11
Days >T10	2	2	2	2
Daily maximum (mm)	196.9	205.7	198.9	232.4
Rain/rain day (mm day^{-1})	13.6	15.5	15.4	17.1

Elevations for the stations increase from left to right (see Table 1 for specific station elevations).

Table 5. Trends in the lower (Q1) and upper (Q3) quartiles and the IQR at RRG06 for the number of days with totals over 25 mm, by season and year, 1937–2013.

	Q1	Q3	IQR
Winter	**−0.619**	**−0.697**	0.321
Spring	−0.32	**0.62**	**−0.435**
Summer		0.293	**0.484**
Autumn	**0.803**	**0.572**	**0.596**
Year	**−0.401**		**0.371**

Correlations significant at $p < 0.05$ are shown in plain font, $p < 0.01$ in bold and $p < 0.001$ in bold and underlined ($n = 57$). Blank cells indicate no significant correlation. Moving window length is 20 years.

was the only season where Q1 went up, but even so, there was a significant increase in the IQR, as a result of a strongly upward trend for Q3. In winter both Q1 and Q3 fell but nevertheless the IQR increased. The overall pattern for the year as a whole was an increase in IQR therefore, with the strongest effect seen in autumn.

3.4. Drought

Notwithstanding some evidence of more intense precipitation recently, greater variability (as shown by significant increases in IQR) implies a trend towards more frequent periods of prolonged drought; and indeed, other than one event in the early 1940s, severe droughts were a feature of the Coweeta climate since the mid-1980s (Figure 3(a)). The major periods of rainfall deficit were more clearly related to the number of heavy falls of rain than to the number of wet days. Whilst, as noted above, there was no significant long-term trends in the number of daily falls over 25 mm, variability clearly increased, matching the pattern for rainfall total (Figure 3(c)).

3.5. Orographic enhancement

Mean rainfall increased with altitude (Table 4). The gradient in precipitation between the lowest and highest gauges (RRG06 and RRG31) was 85 mm per 100 m. The intermediate gauges RRG96 and RRG13 showed differences in the gradient (99 mm (100 m)$^{-1}$ and 60 mm (100 m)$^{-1}$, respectively), likely due to differences in gauge exposure (Swift *et al.*, 1988) or shelter by surrounding trees. Daily rainfall data for ridge top and valley bottom locations was relatively similar in all seasons except autumn, where the

Table 6. Comparison between daily rainfall statistics for the ridge top (RRG31) and valley floor (RRG06) for the period 1959–2012 inclusive.

	Winter	Spring	Summer	Autumn	Annual
Rainfall total ridge	647	621	540	581	2394
Rainfall total	506	480	402	422	1814
valley Gradient [mm (100 m)$^{-1}$]	21	21	20	23	85
Rain days ridge	35	36	40	29	140
Rain days valley	33	35	37	28	134
Gradient [days (100 m)$^{-1}$]	0.3	0.2	0.4	0.1	0.9
Rain per rain day ridge	18.2	17.3	13.4	20.2	17.1
Rain per rain day	15.2	13.9	10.4	15.3	13.6
valley Gradient [mm day^{-1} (100 m)$^{-1}$]	0.4	0.5	0.4	0.7	0.5
Days ≥25 mm ridge	9	8	6	8	31
Days ≥25 mm valley	7	6	4	5	22
Gradient [days (100 m)$^{-1}$]	0.3	0.4	0.3	0.4	1.3

Table 7. Frequency distribution of differences in daily rainfall totals between RRG31 and RRG06 for the period November 1958 through December 2013.

Bins	*n*	%
>5	75	1.1
4	72	1.1
3	158	2.3
2	432	6.4
1	1102	16.3
0	3597	53.1
−1	1098	16.2
−2	147	2.2
<−2	99	1.5

Only rain days (≥0.25 mm) are included ($n = 6780$). The bins indicate the difference (mm) between the high-altitude gauge RRG31 and the valley-bottom gauge RRG06. Positive values show higher rain at altitude and vice versa.

gradient is larger (Table 6). The highest daily rainfall for any Coweeta rain gauge was recorded at the high-elevation gauge RRG31, 232.4 mm on 28 May 1976. There was very little difference in the frequency of rain days at the ridge top and valley bottom gauges, but given higher autumn totals and lower number of rain days, the gradient in rain per rain day was significantly higher in autumn compared to other seasons. The frequency of heavy falls of rain also increased with altitude, although there was little seasonal variation. Whilst totals were often similar for both RRG31 and RRG06 and there were some days where totals were higher at the latter low-altitude gauge, the largest differences in total were always in favour of the high-altitude gauge (Table 7).

3.6. Atmospheric drivers

Given Coweeta's location in the SE United States, strong linkage between the Bermuda High and Coweeta precipitation is to be expected. We employed two indices of atmospheric circulation in relation to the Bermuda High: BHI and WBHI (Diem, 2013). Results reported are for the period 1959–2013 ($n = 55$). Both the BHI and the WBHI were positively related to rainfall totals, number of wet days and the number of daily rainfalls above 25 mm. Total rainfall at RRG06 was positively related to BHI in three seasons ($r > 0.39$ and $p < 0.001$: winter, summer and autumn); and to WBHI in all four seasons ($r > 0.43$, $p < 0.00003$). The same pattern was seen for number of wet days: BHI had significant correlations in three seasons ($r > 0.41$ and $p < 0.002$ for winter, summer and autumn), and WBHI had significant correlations in all four seasons ($r > 0.58$, $p < 0.00001$ for all four seasons). In contrast to Diem (2013), who found a decline in the number of rain days since the 1970s in the Atlanta region, the seasonal correlations for both BH indices from 1959 to 2013 at Coweeta are positive. This may either relate to different rainfall-generation processes being dominant in the mountains compared to the piedmont, or more likely reflect the longer window of analysis used here (Howden *et al.*, 2011). Daily rainfalls totalling more than 25 mm were positively related to BHI in winter and summer ($r > 0.3$, $p < 0.00009$), and to WBHI in all four seasons ($r > 0.36$ and $p < 0.007$).

NAO was a strong atmospheric driver of summer precipitation at Coweeta. Total summer precipitation was positively correlated with the NAO ($r = 0.37$, $p = 0.005$). Using detrended NAO data made no difference in the correlation with summer rainfall ($r = 0.38$). Summers with very high NAO (>0.72, 1 SD above the mean) and those with very low NAO (<−0.87, −1 SD) produced significantly different rainfall totals ($p = 0.002$). Summer NAO declined over time. The summers of 2009–2012 all had a very low NAO, but conditions reversed in summer 2013, with a seasonal total of 708 mm, and nine daily totals over 25 mm. Not only was NAO correlated with rainfall indices, but the strength of the relationship was amplified with altitude (Table 8). With one exception, the regression coefficients were larger at RRG31; however, only four of the six correlations were stronger at the high-altitude site. A very similar pattern was

Table 8. Double orographic enhancement (Burt and Howden, 2013) at Coweeta: regression and correlation coefficients for relationships between the NAO and various rainfall statistics.

	Total rainfall (mm)	Number of rain days	Daily totals ≥25 mm
(a) Regression coefficients			
RRG06 summer	61.0	2.08	1.02
RRG31 summer	76.3	3.04	1.42
RRG06 year	206.2	7.35	3.05
RRG31 year	258.8		4.81
(b) Correlation coefficients			
RRG06 summer	0.370	0.275	0.362
RRG31 summer	0.343	0.378	0.384
RRG06 year	0.365	0.289	0.350
RRG31 year	0.358		0.411

Results for RRG06 and RRG31 only, 1959–2013. Blank cells indicate no significant correlation.

Table 9. Regression and correlation coefficients for relationships between the BHI and various rainfall statistics at RRG06 and RRG31.

	Total rainfall (mm)	Number of rain days	Daily totals ≥25 mm
(a) Regression coefficients			
RRG06 summer	82.1	2.47	1.34
RRG31 summer	122.1	2.87	1.84
RRG06 winter	51.1	2.48	0.75
RRG31 winter	62.8	0.19	0.92
(b) Correlation coefficients			
RRG06 summer	0.533	0.388	0.503
RRG31 summer	0.587	0.382	0.53
RRG06 winter	0.39	0.415	0.301
RRG31 winter	0.381	0.509	0.324

seen using BHI: only one regression coefficient was lower at the high-altitude gauge (number of wet days in winter) and only two results had lower correlation coefficients at the high-altitude gauge (winter totals and number of heavy falls in summer, Table 9).

Winter rainfall was significantly correlated with the average NAO value for the previous calendar year ($r = 0.319$, $p = 0.005$) and the previous summer ($r = 0.23$, $p = 0.04$). The same lagged relationships pertained for daily totals over 25 mm. Much the same pattern of correlations was found at all gauges and the PNA index: total winter rainfall was negatively correlated to the PNA index ($r = -0.29$, $p = 0.023$, $n = 62$), as was spring total rainfall and previous winter's PNA ($r = -0.32$).There was also a positive relationship between for winter PNA and number of rain days ($r = 0.348$, $p = 0.006$), but none for heavy rainfall. The Pacific Ocean indices NINO12 and NINO34 produced very few significant correlations with Coweeta rainfall statistics (RRG06) although the number of wet days in autumn was weakly related to both NINO12 ($r = 0.22$, $p = 0.054$, $n = 76$) and NINO34 ($r = 0.21$, $p = 0.066$).

4. Discussion

Summer was the only season positively correlated with the NAO in the same season (i.e. zero lag); this was seen at all gauges for total and number of days above 25 mm. This matches the results for streamflow found by Coleman and Budikova (2013). During a positive NAO phase, the pressure gradient between the subtropical and polar regions of the North Atlantic intensifies, the Bermuda High extends westward and south-easterly flow advects the moist air masses inland over the southern Appalachians. Coleman and Budikova (2013) suggest that this may generate localized convection and orographic uplift along the east side of the Appalachian ridge. Tropical storms deflected around the Bermuda High provide additional, often very heavy, falls of rain. Negative NAO conditions see the Bermuda High considerably weakened, associated with drier northerly air flow (Coleman and Budikova, 2013; figure 7). The trend since the 1930s has been for summer NAO to decrease but, as noted above, summer rainfall variables at Coweeta also correlate with the detrended NAO index. This gives confidence in a causal relationship, not simply an association related to both variables being collinear with an independent variable, e.g. rising summer temperatures. Since inter-annual variations in summer NAO correlate with Coweeta summer rainfall, there is a straightforward explanation in terms of the strength of the Bermuda High and the associated pressure gradient across the polar front.

Indeed, rainfall models reveal the Bermuda High to be an important predictor of the precipitation regime at Coweeta (*cf* Diem, 2013). At all four gauges, the WBHI was strongly correlated with totals, numbers of wet days and numbers of heavy falls in all four seasons. Of 48 possible correlations (four gauges, four seasons, three rainfall variables), 48 were statistically significant. BHI was less powerful as a predictor (34 significant correlations) because it never correlated with any of the spring rainfall variables. Diem (2013) showed that increased rainfall variability in the southeast United States related to increased variability in the WBHI. Extreme negative values of the WBHI occur when the Bermuda High extends over much of the Southeast and vice versa. Further work is needed to understand why BHI does not predict spring rainfall at Coweeta.

Autumn showed a general pattern of increased precipitation over time, unlike the other seasons where, if there were any trend at all, it tended to be downwards. Autumn totals and numbers of falls above 25 mm showed positive trends at RRG06 and RRG40; all four gauges showed upward trends for mean rain per rain day in autumn. These positive trends in autumn were accompanied by increased variability: given four gauges, three indices of variability (Q1, Q3, IQR) and four variables (total, wet days, falls above 25 mm, T10), autumn showed positive trends for 34 out of a possible 48 correlations. Excluding numbers of wet days, which tended not to be collinear with other variables, there were significant positive trends for 31 out of 36 possibilities. Even so, autumn rainfall was poorly correlated with atmospheric drivers: only number of wet days correlated weakly with NINO12 and NINO34. Notwithstanding a general context of increasing variability, autumn rainfall totals tended to increase, with heavy falls of rain more frequent. During the El Niño portion of ENSO, increased precipitation falls along the Gulf Coast and southeast United States due to a stronger than normal and more southerly polar jet stream. Both summer and autumn NAO declined over time (this could relate to changes in either or both the Bermuda High and the Icelandic Low), which may have enabled a greater influence of Pacific Ocean conditions across the Caribbean and the southeast United States. This merits further attention and, as well as looking for more relevant indices of atmospheric circulation for this region and season, it might be fruitful to analyse objectively derived weather types (Kalnay *et al.*, 1996; Compo *et al.*, 2011) to see why the autumnal rainfall regime has changed at Coweeta (*cf* Diem, 2013, Table 3, which is for summer only). This is relevant since autumn rainfall shows the greatest rate of orographic enhancement of any season (see also below); the long-term increase in autumn rainfall may well have implications for downstream flood generation given the importance of autumnal rainfall for recharge of soil moisture deficits. The results at Coweeta do not accord with those reported in Shepherd *et al.* (2007) because at Coweeta winter and spring have the highest number of days with heavy falls of rain (daily rainfall totals over 25 mm). Even so, the upward trend in autumn for the total of daily falls over 25 mm may well relate to the increase in intense hurricane activity discussed by Shepherd *et al.* (2007). Whilst autumn rainfall was more variable over time (Table 5), there was nevertheless a significant upward trend in the number of extreme rainfall events (as measured by the number of daily totals above 25 mm).

High winter rainfall totals reflect enhanced westerly airflow and the influence of warm moist air from the Gulf of Mexico. A positive PNA is indicative of the strength and location of the East Asian jet stream and, subsequently, the weather it delivers to North America. As the magnitude of the positive PNA increases, the large-scale weather pattern is increasingly meridional which implies a greater transport of heat, moisture and momentum between low and high latitudes over North America.

The strongest, most extensive correlations between the PNA index and precipitation have been observed in winter and early spring (Leathers *et al.*, 1991). Winter was notably the only season with a significant (negative) correlation between rainfall total and the PNA index at RRG06, although there was also a significant correlation between spring rainfall total and PNA in the preceding winter. None of the gauges had a correlation with numbers of daily totals above 25 mm. Both Leathers *et al.* (1991, figure 3) and Yin (1994, figure 7a) confirm that, given its location, Coweeta should have a negative correlation with the PNA index. A positive PNA index sees the polar jet further south and east than usual, resulting in a decrease in precipitation amounts for a large part of central United States including the southern Appalachians. Cyclones are less frequent in this region given changes in track; in addition, polar and arctic continental air masses dominate the region, further decreasing precipitation. With negative PNA index values, the polar front jet is pushed far to the north of its mean position over eastern United States. This allows tropical maritime air masses from the Gulf of Mexico to cross the region more often, increasing precipitation.

The gradient in annual precipitation between the lowest and highest gauges was considerably steeper than any gradients measured in the UK [of which the maximum is 45.8 mm $(100\,\text{m})^{-1}$ in Snowdonia (Unwin, 1969)]. For a group of 19 gauges in the Pacific NW United States, the average gradient was 66.2 mm $(100\,\text{m})^{-1}$ (Burt and Howden, 2013). The result at Coweeta reflects its relatively southern location, its exposure to warm, moist tropical air masses and the steep topography and high elevation locally. Results suggest that autumn has the most favourable conditions conducive to orographic enhancement, but the effect is strong in all seasons. The orographic effect comprises seeder clouds in the form of passing depression systems and feeder clouds in the form of low cloud and fog over the hills; Wilson and Barros (2014) detail the mechanisms involved in this process. In general, the strength of the relationships between NAO, BHI and rainfall are amplified with altitude (Tables 7–9). However, the results are not fully convincing: not all of the significant regression coefficients or correlation coefficients are larger at RRG31, the high-altitude gauge. This weakens the argument for a ‘double orographic enhancement’ effect in that, although the high-elevation site experiences a stronger absolute response to NAO variability (roughly proportional to mean rainfall), there is not necessarily a stronger correlation at altitude too. This implies that the underlying mechanisms are only to some extent more effective at higher altitudes (*cf* Burt and Howden, 2013). This would merit further investigation using hourly recording gauge data and accompanying microphysics measurements (Wilson and Barros, 2014). It is novel that previous results obtained using the NAO index (Burt and Howden, 2013) have been replicated here using BHI.

Observations of double orographic enhancement (Burt and Howden, 2013) at Coweeta underline the importance of changes in atmospheric circulation for rainfall generation. Total autumn rainfall increased in line with a weakening of the Bermuda High, allowing more tropical maritime air masses to pass over the Coweeta region from the south-west. The tendency in other seasons was for frequency and magnitude to decline, in response to long-term trends in atmospheric circulation as measured by the proxies NAO and PNA. The most marked orographic enhancement can be expected when the atmospheric flow is at its strongest but the increase of PNA in winter and the decrease of NAO in summer have had the opposite effect. Further research on orographic enhancement at Coweeta using hourly rainfall data would be beneficial.

5. Conclusions

Long-term trends in daily rainfall at the Coweeta Hydrologic Laboratory reflected hemispheric changes in the global circulation. There has been a tendency for greater variability in the WBHI (Diem, 2013), resulting in wetter wet years and drier dry years. The Bermuda High was, not surprisingly, the main influence on precipitation regime at Coweeta, with atmospheric circulation in the North Atlantic more generally (as indicated by the NAO index) influential in summer. There is, of course, evidence of the influence of air masses moving from the Gulf of Mexico (as indicated by the PNA index) but direct associations with the Pacific Ocean were not generally seen. Further work using synoptic weather types as well as circulation indices like WBHI would seem worthwhile (*cf* Diem, 2013; Burt *et al.*, 2015). The findings are applicable to the wider southern Appalachian Mountains and to other mountainous regions where there is significant orographic enhancement. The use of the BHI as well as the NAO indices to demonstrate double orographic enhancement is novel, helping to confirm the general applicability of the hypothesis (Burt and Howden, 2013). Further work is needed to explore the downward trend in number of rain days in summer and for the year as a whole, not seen in the wet days' data. This may well be an artefact of the data rather than a real change in the occurrence of light rainfall. If it reflects the impact of higher temperatures on rain gauge catch, it would be good to see whether this observation is replicated across widely different climatic regimes.

Acknowledgements

We thank all scientists, technicians and students who have contributed to the long-term climate and hydrology data at Coweeta. Funding for this research was provided by the USDA Forest Service, Southern Research Station; and the National Science Foundation (NSF), Long-Term Ecological Research (LTER) program (award #DEB-0823293). Any opinions, findings, conclusions or recommendations expressed in the material are those of the authors and do not necessarily reflect the views of the USDA or the NSF. We thank Drs Doug Miller and Marshall Shepherd for their thorough reviews of a draft manuscript, and Dr Jeremy Diem for providing the BHI and WBHI data. The figures were drawn by Chris Orton, Design and Imaging Unit, Department of Geography, Durham University, UK. We thank two anonymous referees for their helpful critique of an earlier draft of this paper.

References

Allan RP, Soden BJ. 2008. Atmospheric warming and the amplification of precipitation extremes. *Science* **321**(5895): 1481–1484. https://doi.org/10.1126/science.1160787.

Bulic IH, Kucharski F. 2012. Delayed ENSO impact on spring precipitation over North/Atlantic European region. *Clim. Dyn.* **38**(11–12): 2593–2612. https://doi.org/10.1007/s00382-011-1151-9.

Burnette DJ, Stahle DW. 2014. Historical perspective on the dust bowl drought in the central United States. *Clim. Change* **116**: 479–494.

Burt TP, Howden NJK. 2013. North Atlantic Oscillation amplifies orographic precipitation and river flow in upland Britain. *Water Resour. Res.* **49**(6): 3504–3515. https://doi.org/10.1002/wrcr.20297.

Burt TP, Howden NJK, Worrall F, Whelan MJ. 2008. Importance of long-term monitoring for detecting environmental change: lessons from a lowland river in south east England. *Biogeosciences* **5**(6): 1529–1535.

Burt T, Howden N, Worrall F. 2014. On the importance of very long-term water quality records. *WIREs Water* **1**(1): 41–48.

Burt TP, Jones PD, Howden NJK. 2015. An analysis of rainfall across the British Isles in the 1870s. *Int. J. Climatol.* **35**(10): 2934–2947. https://doi.org/10.1002/joc.4184.

Coleman JSM, Budikova D. 2013. Eastern U.S. summer streamflow during extreme phases of the North Atlantic Oscillation. *J. Geophys. Res. Atmos.* **118**(10): 4181–4193. https://doi.org/10.1002/jgrd.50326.

Compo GP, Whitaker JS, Sardeshmukh PD, Matsui N, Allan RJ, Yin X, Gleason BE, Vose RS, Rutledge G, Bessemoulin P, Bronnimann S, Brunet M, Crouthamel RI, Grant AN, Groisman PY, Jones PD, Kruk MC, Kruger AC, Marshall GJ, Maugeri M, Mok HY, Nordli O, Ross TF, Trigo RM, Wang XL, Woodruff SD, Worley SJ. 2011. The Twentieth Century Reanalysis Project. *Q. J. R. Meteorol. Soc.* **137**(654): 1–28. https://doi.org/10.1002/qj.776.

Diem JE. 2013. Influences of the Bermuda High and atmospheric moistening on changes in summer rainfall in the Atlanta, Georgia region, USA. *Int. J. Climatol.* **33**(1): 160–172. https://doi.org/10.1002/joc.3421.

Folland CK, Knight J, Linderholm HW, Fereday D, Ineson S, Hurrell JW. 2009. The summer North Atlantic Oscillation: past, present, and future. *J. Clim.* **22**(5): 1082–1103. https://doi.org/10.1175/2008JCLI2459.1.

Hartmann D, Klein Tank A, Rustucci M, Alexander L, Bronnimann S, Charabi Y, Dentener F, Dlugokencky E, Easterling D, Kaplan A. 2013. Observations: atmosphere and surface. In *Climate Change 2013: The Physical Science Basis. Contribution of Working Group I to the Fifth Assessment Report of the Intergovernmental Panel on Climate Change*, Stocker TF, Qin D, Plattner G-K, Tignor M, Allen SK, Boschung J, Nauels A, Xia Y, Bex V, Midgley PM (eds). Cambridge University Press: Cambridge, UK and New York, NY.

Hill F, Browning K, Bader M. 1981. Radar and raingauge observations of orographic rain over south Wales. *Q. J. R. Meteorol. Soc.* **107**(453): 643–670.

Howden NJK, Burt TP, Worrall F, Whelan MJ. 2011. Monitoring fluvial water chemistry for trend detection: hydrological variability masks trends in datasets covering fewer than 12 years. *J. Environ. Monit.* **13**(3): 514–521. https://doi.org/10.1039/c0em00722f.

Hurrell JW, VanLoon H. 1997. Decadal variations in climate associated with the North Atlantic Oscillation. *Clim. Change* **36**(3–4): 301–326. https://doi.org/10.1023/A:1005314315270.

Hurrell JW, Kushnir Y, Ottersen G, Visbeck M. 2003. An overview of the North Atlantic Oscillation. In *The North Atlantic Oscillation: Climatic Significance and Environmental Impact*, Hurrell JW, Kushnir Y, Ottersen G, Visbeck M (eds). American Geophysical Union: Washington, D.C. https://doi.org/10.1029/134GM01.

IRI LDEO. 2015. *Indices nino EXTENDED [NINO12, NINO3, NINO34, NINO4] Table*. http://iridl.ldeo.columbia.edu/SOURCES/.Indices/.nino/.EXTENDED/table:/:table/.html (accessed 8 June 2017).

Kalnay E, Kanamitsu M, Kistler R, Collins W, Deaven D, Gandin L, Iredell M, Saha S, White G, Woollen J, Zhu Y, Chelliah M, Ebisuzaki W, Higgins W, Janowiak J, Mo KC, Ropelewski C, Wang J, Leetmaa A, Reynolds R, Jenne R, Joseph D. 1996. The NCEP/NCAR 40-year reanalysis project. *Bull. Am. Meteorol. Soc.* **77**(3): 437–471. https://doi.org/10.1175/1520-0477(1996)077<0437:Tnyrp>2.0.Co;2.

Kaplan A, Cane MA, Kushnir Y, Clement AC, Blumenthal MB, Rajagopalan B. 1998. Analyses of global sea surface temperature 1856–1991. *J. Geophys. Res. Oceans* **103**(C9): 18567–18589. https://doi.org/10.1029/97jc01736.

Karl TR, Knight RW. 1998. Secular trends of precipitation amount, frequency, and intensity in the United States. *Bull. Am. Meteorol. Soc.* **79**(2): 231–241. https://doi.org/10.1175/1520-0477(1998)079<0231:Stopaf>2.0.Co;2.

Laseter SH, Ford CR, Vose JM, Swift LW. 2012. Long-term temperature and precipitation trends at the Coweeta Hydrologic Laboratory, Otto, North Carolina, USA. *Hydrol. Res.* **43**(6): 890–901. https://doi.org/10.2166/Nh.2012.067.

Leathers DJ, Yarnal B, Palecki MA. 1991. The Pacific North-American teleconnection pattern and United-States climate. 1. Regional temperature and precipitation associations. *J. Clim.* **4**(5): 517–528. https://doi.org/10.1175/1520-0442(1991)004<0517:Tpatpa>2.0.Co;2.

Li WH, Li LF, Fu R, Deng Y, Wang H. 2011. Changes to the north Atlantic subtropical high and its role in the intensification of summer rainfall variability in the southeastern United States. *J. Clim.* **24**(5): 1499–1506. https://doi.org/10.1175/2010JCLI3829.1.

Linacre E. 1992. *Climate Data and Resources: A Reference and Guide*. Psychology Press: Routledge, Abingdon, UK.

Maraun D, Osborn TJ, Gillett NP. 2008. United Kingdom daily precipitation intensity: improved early data, error estimates and an update from 2000 to 2006. *Int. J. Climatol.* **28**(6): 833–842. https://doi.org/10.1002/joc.1672.

Meehl GA, Stocker TF, Collins WD, Friedlingstein P, Gaye AT, Gregory JM, Kitoh A, Knutti R, Murphy JM, Noda A, Raper SCB, Watterson IG, Weaver AJ, Zhao Z-C. 2007. Global climate projections. In *Climate Change 2007: The Physical Science Basis, Contribution of Working Group I to the Fourth Assessment Report of the Intergovernmental Panel on Climate Change*, Solomon S, Qin D, Manning M, Chen C, Marquis M, Averyt KB, Tignor M, Miller HL (eds). Cambridge University Press: Cambridge, NY.

NOAA National Weather Service. 2015. *Northern Hemisphere Teleconnection Patterns*. http://www.cpc.ncep.noaa.gov/data/teledoc/telecontents.shtml. (accessed 8 June 2017).

O'Gorman PA, Schneider T. 2009. The physical basis for increases in precipitation extremes in simulations of 21st-century climate change. *Proc. Natl. Acad. Sci. USA* **106**(35): 14773–14777. https://doi.org/10.1073/pnas.0907610106.

Osborn TJ, Hulme M, Jones PD, Basnett TA. 2000. Observed trends in the daily intensity of United Kingdom precipitation. *Int. J. Climatol.* **20**(4): 347–364. https://doi.org/10.1002/(Sici)1097-0088(20000330)20:4<347::Aid-Joc475>3.0.Co;2-C.

Prat OP, Barros AP. 2010. Ground observations to characterize the spatial gradients and vertical structure of orographic precipitation – experiments in the inner region of the Great Smoky Mountains. *J. Hydrol.* **391**(1–2): 143–158. https://doi.org/10.1016/j.jhydrol.2010.07.013.

Shepherd JM, Grundstein A, Mote TL. 2007. Quantifying the contribution of tropical cyclones to extreme rainfall along the coastal southeastern United States. *Geophys. Res. Lett.* **34**(23): L23810. https://doi.org/10.1029/2007gl031694.

Stahle DW, Cleaveland MK. 1992. Reconstruction and analysis of spring rainfall over the southeastern US for the past 1000 years. *Bull. Am. Meteorol. Soc.* **73**(12): 1947–1961.

Swank WT, Crossley DA (eds). 1988. *Forest Hydrology and Ecology at Coweeta*. Ecological Studies, Vol. **66**. Springer-Verlag: New York, NY.

Swift LW, Cunningham GB, Douglass JE. 1988. Climate and hydrology. In *Forest Hydrology and Ecology at Coweeta*. Ecological Studies, Vol. **66**, Swank WT, Crossley DA (eds). Springer-Verlag: New York, NY.

UEA CRU. 2015. *North Atlantic Oscillation (NAO)*. https://crudata.uea.ac.uk/cru/data/nao/ (accessed 8 June 2017).

Unwin D. 1969. The areal extension of rainfall records: an alternative model. *J. Hydrol.* **7**(4): 404–414.

Wang H, Fu R, Kumar A, Li WH. 2010. Intensification of summer rainfall variability in the southeastern United States during recent decades. *J. Hydrometeorol.* **11**(4): 1007–1018. https://doi.org/10.1175/2010JHM1229.1.

Wilson AM, Barros AP. 2014. An investigation of warm rainfall microphysics in the southern Appalachians: orographic enhancement via low-level seeder–feeder interactions. *J. Atmos. Sci.* **71**(5): 1783–1805. https://doi.org/10.1175/Jas-D-13-0228.1.

Yin ZY. 1994. Moisture condition in the south-eastern USA and teleconnection patterns. *Int. J. Climatol.* **14**(9): 947–967. https://doi.org/10.1002/joc.3370140902.

